

# Detailed Next-to-Leading Order Analysis of Deep Inelastic Neutrino Induced Charm Production off Strange Sea Partons

M. Glück, S. Kretzer and E. Reya

Institut für Physik, Universität Dortmund  
D-44221 Dortmund, Germany

## Abstract

Neutrino induced deep inelastic charm production off strange sea partons in the nucleon is studied in the framework of the  $\overline{\text{MS}}$  fixed flavor factorization scheme. The momentum ( $z$ ) distributions of the produced D mesons as calculated in the next-to-leading order QCD analysis are presented and compared to their leading order counterparts. Perturbative stability within this formalism is demonstrated and the compatibility of recent next-to-leading order (NLO) strange quark distributions with available dimuon data is investigated. Our NLO ( $\overline{\text{MS}}$ ) results provide, for the first time, the tools required for a consistent and complete NLO ( $\overline{\text{MS}}$ ) analysis of charged current dimuon data in order to extract the strange sea density in NLO. It is furthermore shown that the absolute predictions of radiatively (dynamically) generated strange sea densities are in agreement with all present measurements.

Recent attempts [1, 2] to determine the strange sea content of the nucleon,  $s(x, Q^2)$ , from a next-to-leading order (NLO) QCD analysis of neutrino induced charm production (opposite-sign dimuon events) were undertaken in the framework of the NLO formalism of [3]. In this formalism one considers, in addition to the leading order (LO) process  $W^+s \rightarrow c$ , etc., the  $W^+g \rightarrow c\bar{s}$  gluon fusion contribution with  $m_s \neq 0$ , i.e. one employs a finite mass regularization and subtracts from it that (collinear) part which is already contained in the renormalized,  $Q^2$ -dependent  $s(x, Q^2)$ . In a previous publication [4] we have started a study of NLO QCD effects based on the conventional  $\overline{\text{MS}}$  factorization scheme where the mass of the strange quark is neglected ( $m_s = 0$ ) and the corresponding mass singularities are dimensionally regularized [5]. Such an analysis is imperative in connection with all those NLO parton distributions and cross sections given in this, most frequently utilized, massless  $\overline{\text{MS}}$  factorization scheme. The analysis in [4] was incomplete, however, in the sense of not addressing the detailed momentum distributions of the produced  $c$ -quark (D-meson) utilized in [1, 2]. The present paper is devoted to this issue and the relevant expressions are now calculated in their full differential form, by extending the original inclusive analysis in [5].

The formulae and notations of [4] will be strictly taken over everywhere, being extended merely by the introduction of the fractional charm momentum variable  $\zeta \equiv p_c \cdot p_N / q \cdot p_N$ , i.e.  $H_i^{q,g}(\xi', \mu^2, \lambda)$  in [4] will be replaced by  $H_i^{q,g}(\xi', \zeta, \mu^2, \lambda)$  where the fermionic and gluonic NLO coefficient functions  $H_{i=1,2,3}^q$  and  $H_i^g$  for heavy quark (charm) production derive from the subprocess  $W^+s \rightarrow cg$  (together with the virtual vertex correction to  $W^+s \rightarrow c$ ) and  $W^+g \rightarrow c\bar{s}$ , respectively. Furthermore,  $d^2\sigma^{\nu(\bar{\nu})}/dx dy$  in [4] will be replaced by  $d^3\sigma^{\nu(\bar{\nu})}/dx dy dz$  with the relevant semi-inclusive structure functions, describing the momentum distributions of the produced D-mesons, being obtained from a convolution with the charm fragmentation function  $D_c(z)$ ,<sup>1</sup>

---

<sup>1</sup>Instead of  $z \equiv p_D \cdot p_N / q \cdot p_N$ , it is customary to use [1, 2, 7]  $z_p \equiv p_D / p_D^{max}$  which differs only marginally from  $z$  in the relevant experimental region ( $z \gtrsim 0.05$ ).

$$\begin{aligned}
\mathcal{F}_i^c(x, z, Q^2) &= s'(\xi, \mu_F^2) D_c(z) \\
&+ \frac{\alpha_s(\mu_F^2)}{2\pi} \int_{\xi}^1 \frac{d\xi'}{\xi'} \int_{\max(z, \zeta_{\min})}^1 \frac{d\zeta}{\zeta} \left[ H_i^q(\xi', \zeta, \mu_F^2, \lambda) s'(\frac{\xi}{\xi'}, \mu_F^2) \right. \\
&+ \left. H_i^g(\xi', \zeta, \mu_F^2, \lambda) g(\frac{\xi}{\xi'}, \mu_F^2) \right] D_c(\frac{z}{\zeta}) .
\end{aligned} \tag{1}$$

where  $\mathcal{F}_1^c \equiv F_1^c$ ,  $\mathcal{F}_3^c \equiv F_3^c/2$ ,  $\mathcal{F}_2^c \equiv F_2^c/2\xi$  with  $\xi = x(1 + m_c^2/Q^2)$ ,  $\zeta_{\min} = m_c^2/\hat{s} = (1 - \lambda)\xi'/(1 - \lambda\xi')$  and  $\lambda = Q^2/(Q^2 + m_c^2)$ . The  $H_i^{q,g}$  are given in the Appendix and our choice for the factorization scale will be  $\mu_F^2 = Q^2 + m_c^2$ , although the results are not very sensitive to this specific choice. The fractional momentum of the D-meson is denoted by  $z \equiv p_D \cdot p_N / q \cdot p_N$  and the (factorization scale independent) charm fragmentation function is taken as [6]

$$D_c(z) = N \left\{ z \left[ 1 - z^{-1} - \varepsilon_c/(1 - z) \right]^2 \right\}^{-1} \tag{2}$$

with the normalization constant  $N$  being related to  $\varepsilon_c$  via  $\int_0^1 dz D_c(z) = 1$ , while  $\varepsilon_c$  itself will be fitted to the measured  $z$ -distributions. One can infer these distributions by utilizing the LO version of eq. (1) which has a simple factorized form

$$\frac{d^3 \sigma_{LO}^{\nu(\bar{\nu})}}{dx dy dz} = \frac{d^2 \sigma_{LO}^{\nu(\bar{\nu})}}{dx dy} D_c(z) \tag{3}$$

together with the corresponding parameters in the LO analysis [7] of which  $\varepsilon_c^{LO} = 0.20 \pm 0.04$  is the most relevant now [8]. It should be mentioned that the CCFR group has also performed a 'NLO' analysis [1] of their dimuon data using the simple factorized LO expression in eq. (3) instead of the correct (convoluted) NLO expressions in (1), which are just the finite-mass extensions of the well known NLO results for light (massless) quarks [9]. We shall analyze the 'data' [7] as parametrized in LO by eq. (3).

To simplify the presentation of our results we define [4]

$$\xi s(\xi, z, Q^2)_{eff} \equiv \frac{1}{2} \frac{\pi(1 + Q^2/M_W^2)^2}{G_F^2 M_N E_\nu} |V_{cs}|^{-2} \frac{d^3 \sigma^{(c\bar{s})}}{dx dy dz} \tag{4}$$

which has also been studied experimentally [1] and where the superscript  $c\bar{s}$  refers just to the CKM non-suppressed ( $V_{cs}$ ) component of  $s' \equiv |V_{cs}|^2 s + |V_{cd}|^2 (d + u)/2$  in eq. (1).

In LO the cross section in (4) reduces to [4], cf. eqs. (1) and (3),

$$\xi s(\xi, z, Q^2)_{eff} = \left(1 - \frac{m_c^2}{2M_N E_\nu \xi}\right) \xi s(\xi, \mu^2) D_c(z) \quad . \quad (5)$$

Our LO and NLO results for  $s_{eff}$  are shown in figs. 1 and 2 using the GRV [10] and CTEQ4 [11] parton densities, respectively. It should be emphasized that the 'data' on  $d^3\sigma/dxdydz$  are well reproduced in NLO provided one selects a harder nonperturbative charm fragmentation function  $D_c(z)$  corresponding to  $\varepsilon_c^{NLO} = 0.06$  in eq. (2) as expected to be necessary for compensating the softening effects due to the NLO  $\mathcal{O}(\alpha_s)$  corrections (as is evident from comparing the dashed and solid curves in figs. 1 and 2). Similar  $\mathcal{O}(\alpha_s)$  softening effects due to gluon bremsstrahlung in  $e^+e^- \rightarrow DX$  imply [12, 13]  $\varepsilon_c^{NLO} = 0.06 \pm 0.03$ . It is interesting to note that similar values for  $\varepsilon_c^{NLO}$ , i.e.  $\varepsilon_c^{NLO} \simeq 0.06$  are obtained in NLO by comparing the predictions of the NLO perturbative fixed order QCD corrections to  $e^+e^- \rightarrow DX$ , based on the corresponding cross sections in [14], with the ARGUS data [8, 15] ( $\sqrt{s} \simeq 10$  GeV).

Apart from the very large  $z$  region ( $z \gtrsim 0.8$ ), where the perturbative  $\ln(1-z)$  singularities have to be resummed [16] and nonperturbative higher twist contributions [17] will play a dominant role, our LO and NLO results in figs. 1 and 2 show a remarkable perturbative stability throughout the experimentally relevant  $z$  and  $x$  region ( $z \lesssim 0.8$ ,  $0.01 \lesssim x \lesssim 0.4$ ) for both sets of parton densities, despite the fact that we have (arbitrarily) fixed  $m_c = 1.5$  GeV in LO and NLO. It should be reemphasized that a proper utilization of the corresponding LO and NLO parton densities and coupling constants (and possibly  $m_c$ ) is essential for the observed perturbative stability of the physical cross sections in eqs. (1), (4) and (5). The results in fig. 1 support the dynamically predicted  $s(x, Q^2)$ , generated purely radiatively from  $s(x, \mu^2) = 0$  at  $\mu_{LO, NLO}^2 = 0.23, 0.34$  GeV<sup>2</sup> [10]. On the other hand, the CTEQ4 densities [11] overshoot somewhat the shaded 'data' band due to the larger strange sea densities.

The observed perturbative stability, as shown for example in fig. 1, can possibly be improved by adopting a different charm mass in LO and NLO, e.g.  $m_c = 1.3$  GeV and  $m_c = 1.7$  GeV, respectively, following refs. [1, 2]. The observed variations of the LO and

total NLO results are shown in fig. 3.

In order to determine the NLO strange sea density, the CCFR collaboration [1, 2] employed, as discussed at the beginning, the NLO mass-regulated ( $m_s \neq 0$ )  $W^+g \rightarrow c\bar{s}$  gluon fusion contribution within the ACOT framework [3] where the NLO  $\mathcal{O}(\alpha_s)$  quark-initiated contribution ( $W^+s \rightarrow cg$ ) is disregarded (since it has not been calculated yet for  $m_s \neq 0$ ). An explicit (more differential) calculation of this gluon-initiated production process along the lines of [3] shows [18] that  $d^3\sigma/dxdydz$  becomes insensitive to  $m_s$  provided one chooses  $m_s \lesssim 200$  MeV, as is usually done [1, 2], and practically coincides with our  $\overline{\text{MS}}$  results, e.g. the dashed-dotted curves in fig. 1. Moreover, these results depend very little on the specific choice of the initial gluon density for the experimentally relevant  $(x, Q^2)$  domain, as is obvious from the dashed-dotted curves in figs. 1 and 2; the gluon density, obtained in the original CCFR analysis [1, 2], gives again a very similar result. It should, however, be noted that CCFR [1] approximated the full convolutions of the NLO gluonic contribution in eq. (1) by a factorized expression similar to the one in eq. (3) while keeping the LO  $D_c(z)$  with  $\varepsilon_c^{LO} \simeq 0.20$ . This 'approximated' factorized expression yields rather different  $z$ - and  $x$ -distributions. Despite the fact that such a factorized NLO approach is theoretically not justified, this inconsistency could be partly 'compensated' by choosing a different value for  $\varepsilon_c$  (and possibly also for  $m_c$ ). In the latter case the extraction of  $s_{NLO}$  becomes rather ambiguous, since the utilized value of  $\varepsilon_c$  cannot be consistently obtained within an analogous NLO analysis of, say,  $e^+e^- \rightarrow DX$ . On top of this comes the contribution from the NLO quark-initiated subprocess  $W^+s \rightarrow cg$  and the NLO vertex correction to  $W^+s \rightarrow c$ , so far neglected by the CCFR analysis [1, 2], which is not negligible according to the dotted curves in figs. 1 and 2. It is thus clear that a consistent and complete NLO-reanalysis of the CCFR dimuon data would certainly be worthwhile.

For illustration we finally compare the NLO strange sea density inferred by the CCFR collaboration [1] with their LO one in fig. 4, where the GRV94 and CTEQ4 strange densities are also shown at  $Q^2 = 4$  and  $22 \text{ GeV}^2$ . The three different strange sea densities are

comparable in the limited  $x$ -domain of the CCFR dimuon data at fixed  $Q^2$  (as indicated). Outside this region the enhancement of the 'extracted'  $s_{NLO}(x, Q^2)$  with respect to, say, the GRV  $s_{NLO}$  should not be taken too literally since the extraction beyond the measured region depends on the assumed input  $x$ -shape as well as on the  $Q^2$ -evolution.<sup>2</sup> On the other hand the excess of the LO/NLO CTEQ4 predictions over the CCFR 'data' band (as extracted in LO) in fig. 2 is caused by the strong enhancement of the CTEQ4 strange quark densities with respect to the LO/NLO GRV ones, in particular for  $x \gtrsim 0.03$ .

To summarize, we have calculated and analyzed within the  $\overline{\text{MS}}$  fixed flavor scheme the momentum ( $z$ ) distributions  $d^3\sigma/dxdydz$  of the  $D$  mesons produced in neutrino induced deep inelastic charm production off strange sea partons (opposite-sign dimuon events) according to the quark- and gluon-initiated NLO subprocesses  $W^+s \rightarrow cg$  (together with the vertex correction to the LO Born process  $W^+s \rightarrow c$ ) and  $W^+g \rightarrow c\bar{s}$ , respectively. Perturbative LO/NLO stability within this formalism has been obtained in the safe  $z \lesssim 0.8$  region and the compatibility of recent LO and NLO strange quark sea densities with available CCFR dimuon data [1, 7] has been investigated. We studied also the mass-regulated ( $m_s \neq 0$ )  $W^+g \rightarrow c\bar{s}$  gluon fusion contribution within the ACOT framework [3], originally used by CCFR for extracting a NLO strange sea density [1] from their dimuon data, where the NLO  $\mathcal{O}(\alpha_s)$  quark-initiated  $W^+s \rightarrow cg$  contribution is disregarded. This  $m_s \neq 0$  gluon initiated contribution turns out to be insensitive to  $m_s$  provided one chooses, as usual,  $m_s \lesssim 200$  MeV and practically coincides with our  $\overline{\text{MS}}$  results [18]. Nevertheless the CCFR NLO analysis [1] of the dimuon data for extracting  $s_{NLO}(x, Q^2)$  is inconsistent due to the use of a theoretically unjustified 'approximated' factorized expression in  $x$  and  $z$  for  $d^3\sigma^{\nu(\bar{\nu})}/dxdydz$ , as well as incomplete due to the neglect of the quark-initiated  $\mathcal{O}(\alpha_s)$  contribution. A consistent and complete NLO-reanalysis of the CCFR dimuon

---

<sup>2</sup> It should be noted that CCFR has assumed a constant value for

$$\kappa(Q^2) \equiv \int_0^1 [xs(x, Q^2) + x\bar{s}(x, Q^2)] dx \Big/ \int_0^1 [x\bar{u}(x, Q^2) + x\bar{d}(x, Q^2)] dx \quad ,$$

using  $\kappa(Q^2) \simeq 0.48$ . This is partly responsible for an enhancement of  $s(x, Q^2)$  at smaller values of  $Q^2$ , since a LO/NLO QCD  $Q^2$ -evolution gives  $\kappa(4 \text{ GeV}^2)/\kappa(20 \text{ GeV}^2) \simeq 0.8$ .

data, using the fully differential and complete NLO ( $\overline{\text{MS}}$ ) contributions as presented in this article, would therefore be worthwhile.

## Acknowledgements

This work has been supported in part by the 'Bundesministerium für Bildung, Wissenschaft, Forschung und Technologie', Bonn.

## Appendix

The fermionic NLO ( $\overline{\text{MS}}$ ) coefficient functions  $H_i^q$  for heavy quark (charm) production in eq. (1), calculated from the subprocess  $W^+s \rightarrow gc$  and the vertex correction to  $W^+s \rightarrow c$  are given by

$$\begin{aligned}
H_1^q(\xi, \zeta, \mu_F^2, \lambda) = & \delta(1-\zeta) \left\{ P_{qq}^{(0)}(\xi) \ln \frac{Q^2 + m_c^2}{\mu_F^2} \right. \\
& + \frac{4}{3} \left[ 1 - \xi + (1-\xi) \ln \frac{(1-\xi)^2}{\xi(1-\lambda\xi)} - 2\xi \frac{\ln \xi}{1-\xi} + 2\xi \left( \frac{1}{1-\xi} \ln \frac{(1-\xi)^2}{1-\lambda\xi} \right)_+ \right] \Big\} \\
& + \frac{4}{3} \left\{ -\delta(1-\xi)\delta(1-\zeta) \left[ \frac{1}{2} \left( \frac{1+3\lambda}{\lambda} K_A + \frac{1}{\lambda} \right) + 4 + \frac{\pi^2}{3} \right] \right. \\
& + \frac{1-\xi}{(1-\zeta)_\oplus} + (1-\zeta) \left( \frac{1-\lambda\xi}{1-\xi} \right)^2 \left[ \frac{1-\xi}{(1-\lambda\xi)^2} \right]_+ \\
& + 2 \frac{\xi}{(1-\xi)_+} \frac{1}{(1-\zeta)_\oplus} \left[ 1 - (1-\zeta) \frac{1-\lambda\xi}{1-\xi} \right] \\
& \left. + 2 \xi \left[ 1 - (1-\zeta) \frac{1-\lambda\xi}{1-\xi} \right] \right\} \quad (\text{A1})
\end{aligned}$$

$$\begin{aligned}
H_2^q(\xi, \zeta, \mu_F^2, \lambda) = & H_1^q(\xi, \zeta, \mu_F^2, \lambda) + \frac{4}{3} \left\{ \delta(1-\xi)\delta(1-\zeta) K_A \right. \\
& \left. - 2 \left( \xi(1-3\lambda) \left[ 1 - (1-\zeta) \frac{1-\lambda\xi}{1-\xi} \right] + (1-\lambda) \right) \right\} \quad (\text{A2})
\end{aligned}$$

$$H_3^q(\xi, \zeta, \mu_F^2, \lambda) = H_1^q(\xi, \zeta, \mu_F^2, \lambda) + 2 \frac{4}{3} \left\{ (1-\xi) \left[ 1 - (1-\zeta) \frac{1-\lambda\xi}{1-\xi} \right] - (1-\lambda\xi) \right\} \quad (\text{A3})$$

with  $K_A = \frac{1}{\lambda}(1-\lambda) \ln(1-\lambda)$  ,  $P_{qq}^{(0)}(\xi) = \frac{4}{3} \left( \frac{1+\xi^2}{1-\xi} \right)_+$  and where the distributions are defined by

$$\int_0^1 d\xi \frac{f(\xi)}{(1-\xi)_+} = \int_0^1 d\xi \frac{f(\xi) - f(1)}{1-\xi} , \quad \int_{\zeta_{min}}^1 d\zeta \frac{f(\zeta)}{(1-\zeta)_\oplus} = \int_{\zeta_{min}}^1 d\zeta \frac{f(\zeta) - f(1)}{1-\zeta} \quad (\text{A4})$$

with  $\zeta_{min} = (1-\lambda)\xi/(1-\lambda\xi)$ . When integrated over  $\zeta$ , these results reduce to the final inclusive results obtained in [4, 5], i.e.

$$H_i^q(\xi, \mu_F^2, \lambda) = \int_{\zeta_{min}}^1 d\zeta H_i^q(\xi, \zeta, \mu_F^2, \lambda) \quad . \quad (\text{A5})$$



The gluonic NLO ( $\overline{\text{MS}}$ ) coefficient functions  $H_i^g$  for heavy quark (charm) production in eq. (1), as calculated from the subprocess  $W^+g \rightarrow c\bar{s}$ , are given by

$$\begin{aligned}
H_i^g(\xi, \zeta, \mu_F^2, \lambda) &= \delta(1 - \zeta) \left\{ P_{qg}^{(0)}(\xi) \left[ \ln \frac{Q^2 + m_c^2}{\mu_F^2} + \ln \frac{(1 - \xi)^2}{\xi(1 - \lambda\xi)} \right] + \xi(1 - \xi) \right\} \\
&+ \left[ \frac{1}{(1 - \zeta)_\oplus} + \frac{1}{\zeta} \right] P_{qg}^{(0)}(\xi) + h_i^g(\xi, \zeta, \lambda)
\end{aligned} \tag{A6}$$

where

$$\begin{aligned}
h_1^g(\xi, \zeta, \lambda) &= -\frac{\xi^2}{\zeta^2}(1 - \lambda)(1 - 2\lambda) + \frac{2\xi}{\zeta}(1 - \lambda)(1 - 2\lambda\xi) \\
&+ 2\xi\lambda(1 - \lambda\xi) - 1
\end{aligned} \tag{A7}$$

$$\begin{aligned}
h_2^g(\xi, \zeta, \lambda) &= \frac{\xi^2}{\zeta^2}(1 - \lambda)(1 - 6\lambda + 6\lambda^2) + \frac{6\lambda\xi}{\zeta}(1 - \lambda)(1 - 2\lambda\xi) \\
&+ \lambda[6\lambda\xi(1 - \lambda\xi) - 1]
\end{aligned} \tag{A8}$$

$$h_3^g(\xi, \zeta, \lambda) = \frac{\xi^2}{\zeta^2}(1 - \lambda)(1 - 2\lambda) - \frac{2}{\zeta}[P_{qg}^{(0)}(\xi) + \xi(1 - \xi - \lambda\xi)(1 - \lambda)] \tag{A9}$$

with  $P_{qg}^{(0)}(\xi) = \frac{1}{2}[\xi^2 + (1 - \xi)^2]$  and the  $\oplus$  distribution is defined in (A4). When integrated over  $\zeta$ , these results reduce to the final inclusive results obtained in [4, 5], i.e.

$$H_i^g(\xi, \mu_F^2, \lambda) = \int_{\zeta_{min}}^1 d\zeta H_i^g(\xi, \zeta, \mu_F^2, \lambda) \quad . \tag{A10}$$

# References

- [1] A. O. Bazarko et al., CCFR collab., Z. Phys. C65 (1995) 189.
- [2] A. O. Bazarko, Ph. D. thesis, Columbia University, Nevis-285 (1994).
- [3] M. A. G. Aivazis, J. C. Collins, F. I. Olness and W.-K. Tung, Phys. Rev. D50 (1994) 3102.
- [4] M. Glück, S. Kretzer and E. Reya, Phys. Lett. B380 (1996) 171.
- [5] T. Gottschalk, Phys. Rev. D23 (1981) 56.
- [6] C. Peterson et al., Phys. Rev. D27 (1983) 105.
- [7] S. A. Rabinowitz et al., CCFR collab., Phys. Rev. Lett. 70 (1993) 134.
- [8] H. Albrecht et al., ARGUS collab., Phys. Rep. 276 (1996) 223.
- [9] G. Altarelli, R. K. Ellis, G. Martinelli and S.-Y. Pi, Nucl. Phys. B160 (1979) 301;  
W. Furmanski and R. Petronzio, Z. Phys. C11 (1982) 293.
- [10] M. Glück, E. Reya and A. Vogt, Z. Phys. C67 (1995) 433.
- [11] H. L. Lai et al., CTEQ collab., Phys. Rev. D55 (1997) 1280.
- [12] J. Chrin, Z. Phys. C36 (1987) 163;  
S. Bethke, *ibid.* C29 (1985) 175.
- [13] Particle Data Group, J. J. Hernández et al., Phys. Lett. B239 (1990) 1.
- [14] P. Nason and B. R. Webber, Nucl. Phys. B421 (1994) 473, and references therein.
- [15] H. Albrecht et al., ARGUS collab., Z. Phys. C52 (1991) 353.
- [16] B. Mele and P. Nason, Nucl. Phys. B361 (1991) 626.
- [17] P. Nason and B. R. Webber, CERN-TH/96-290, and references therein.
- [18] S. Kretzer and I. Schienbein, Univ. Dortmund report DO-TH 97/02 (to appear).

## Figure Captions

**Fig. 1** The predicted  $\xi s(\xi, z, Q^2)_{eff}$  in eqs. (4) and (5) as calculated in LO [NLO] using the dynamical (GRV) parton distributions of ref. [10] and the charm fragmentation functions in eq. (2) corresponding to  $\varepsilon_c = 0.20$  [0.06]. The individual NLO quark- and gluon-initiated contributions derive in an obvious way from eq. (1). The charm mass has been (arbitrarily) fixed in LO and NLO,  $m_c = 1.5$  GeV. The shaded band represents the 'data' as extracted from [7] via eq. (3).

**Fig. 2** Same as fig. 1 but using the LO CTEQ4L and the NLO ( $\overline{\text{MS}}$ ) CTEQ4M parton densities [11].

**Fig. 3** LO and total NLO predictions using different values for  $m_c$  (thin curves). The LO and NLO results for  $m_c = 1.5$  GeV (thick curves) are the same as the corresponding ones in fig. 1. The predictions are based on the GRV densities [10]. The shaded experimental 'data' band corresponds, however, to  $m_c = 1.3$  GeV as utilized in LO in [1, 7] and is the same as in fig. 1.

**Fig. 4** Strange sea densities in LO and NLO at  $Q^2 = 4 \text{ GeV}^2$  and  $Q^2 = 22 \text{ GeV}^2$  according to CCFR [1] and CTEQ4 [11]. The GRV strange densities [10] refer to absolute QCD predictions since they have been generated purely radiatively from a vanishing input  $s(x, \mu_{LO,NLO}^2) = 0$ . The NLO CCFR strange density corresponds to the choice of the factorization scale  $Q^2 + m_c^2$  in Table 5 of ref. [1]. The actual  $x$ -ranges covered by the CCFR data [7] at these fixed values of  $Q^2$  are indicated.

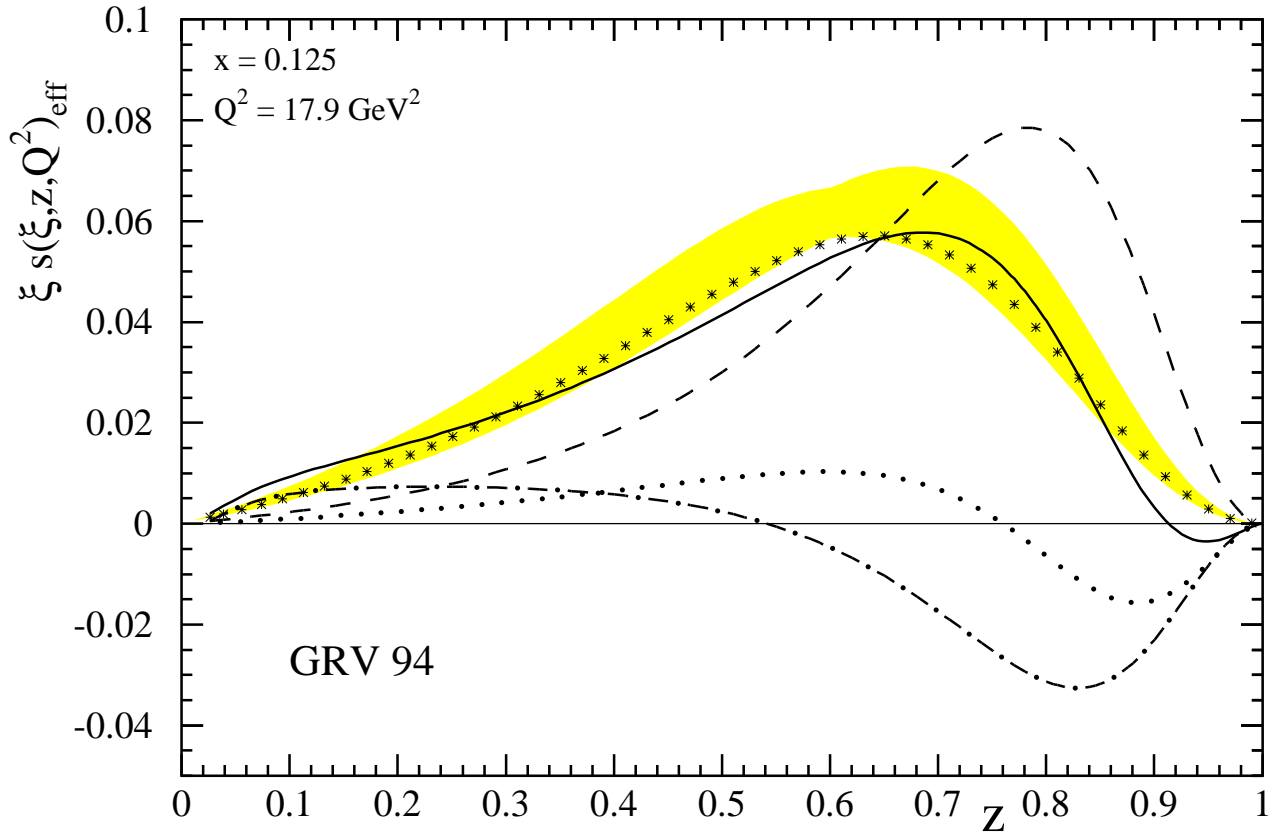
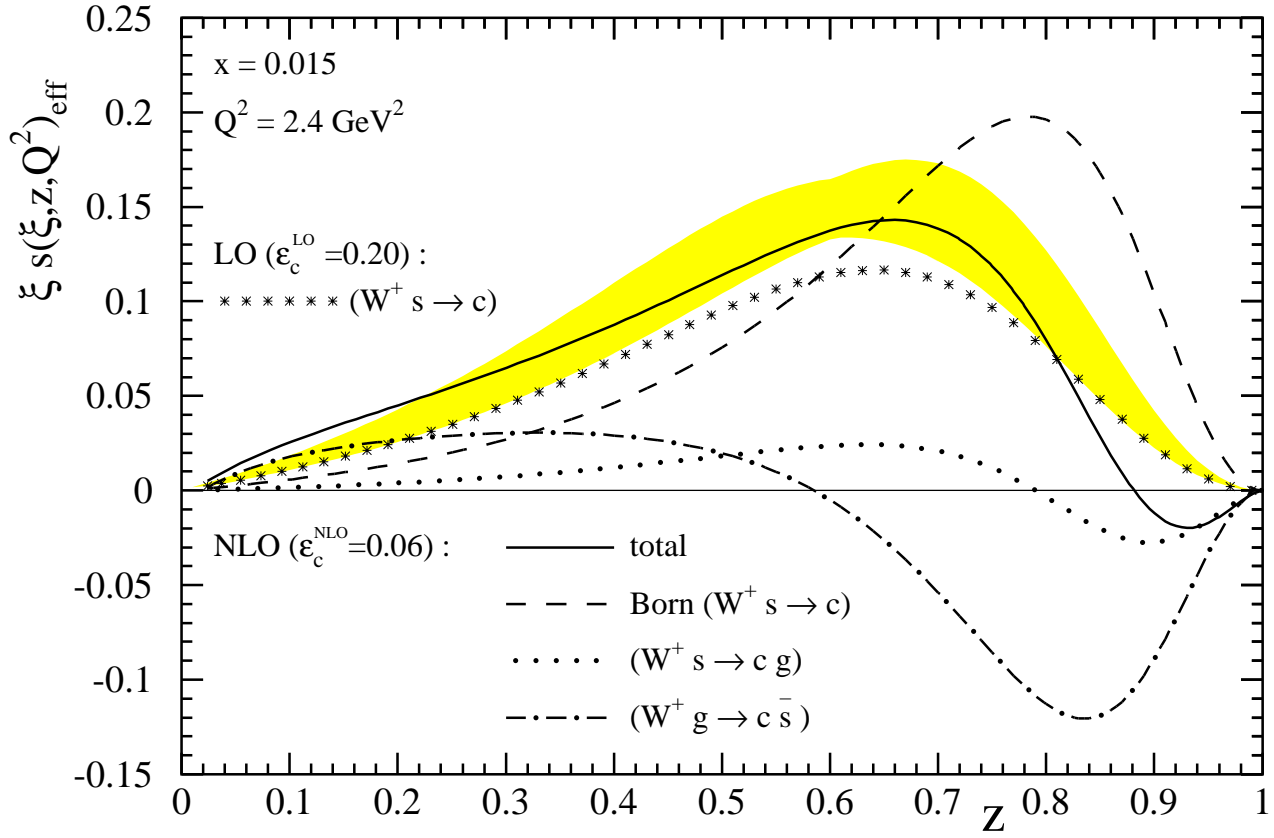


Fig. 1

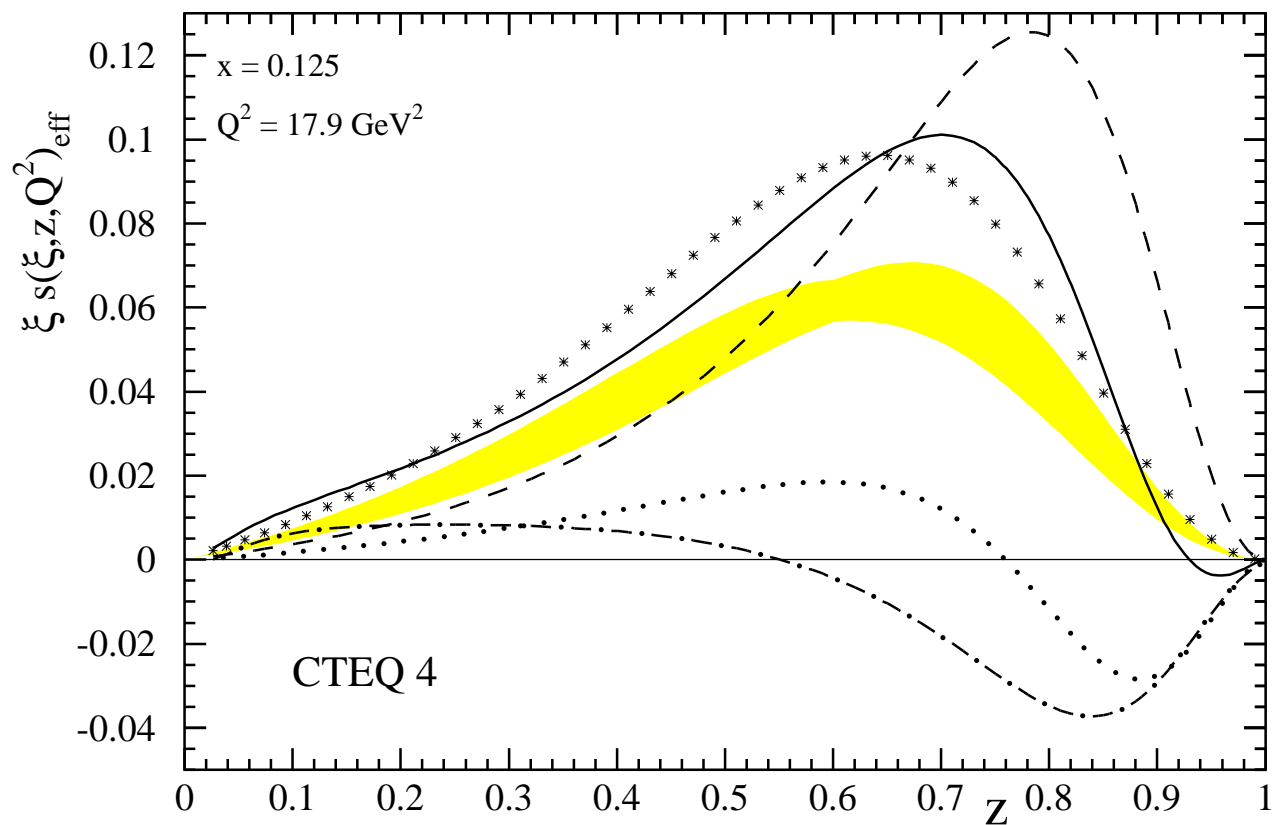
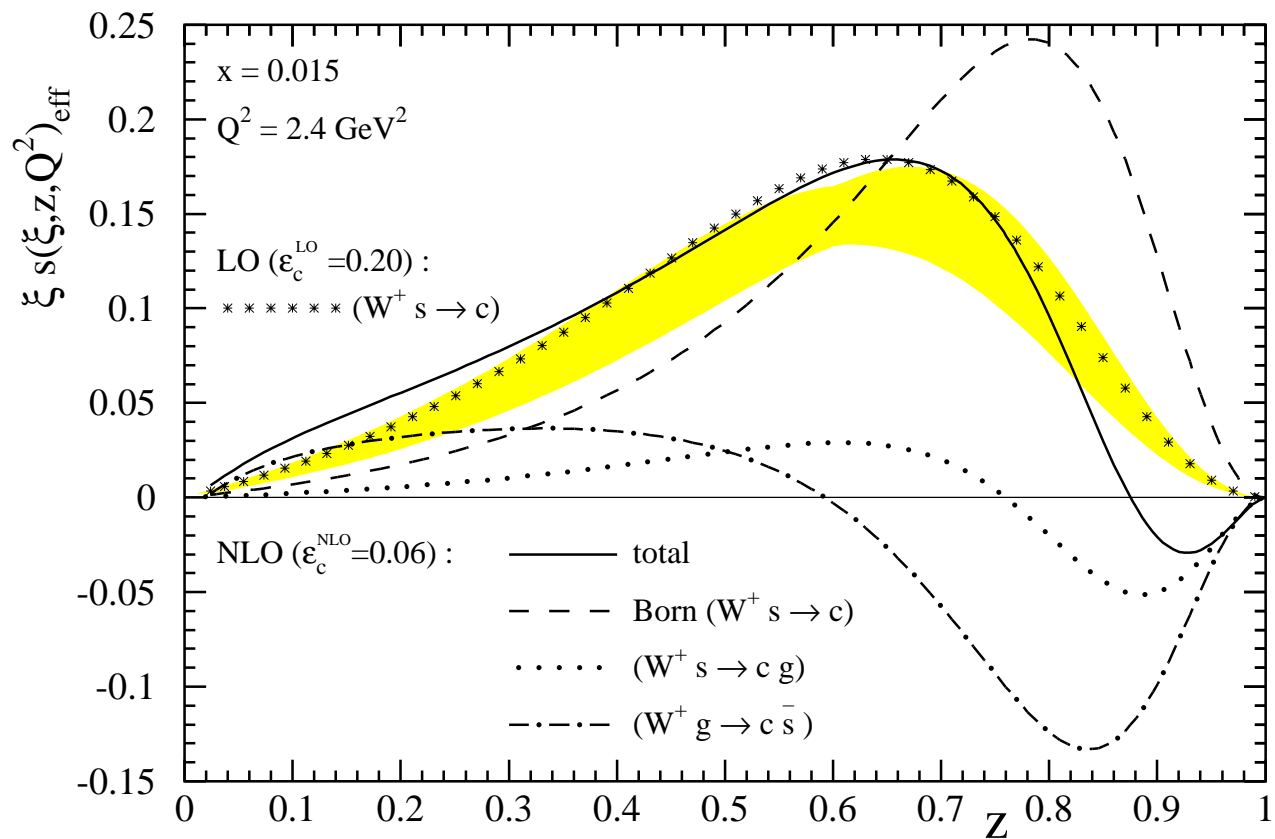


Fig. 2

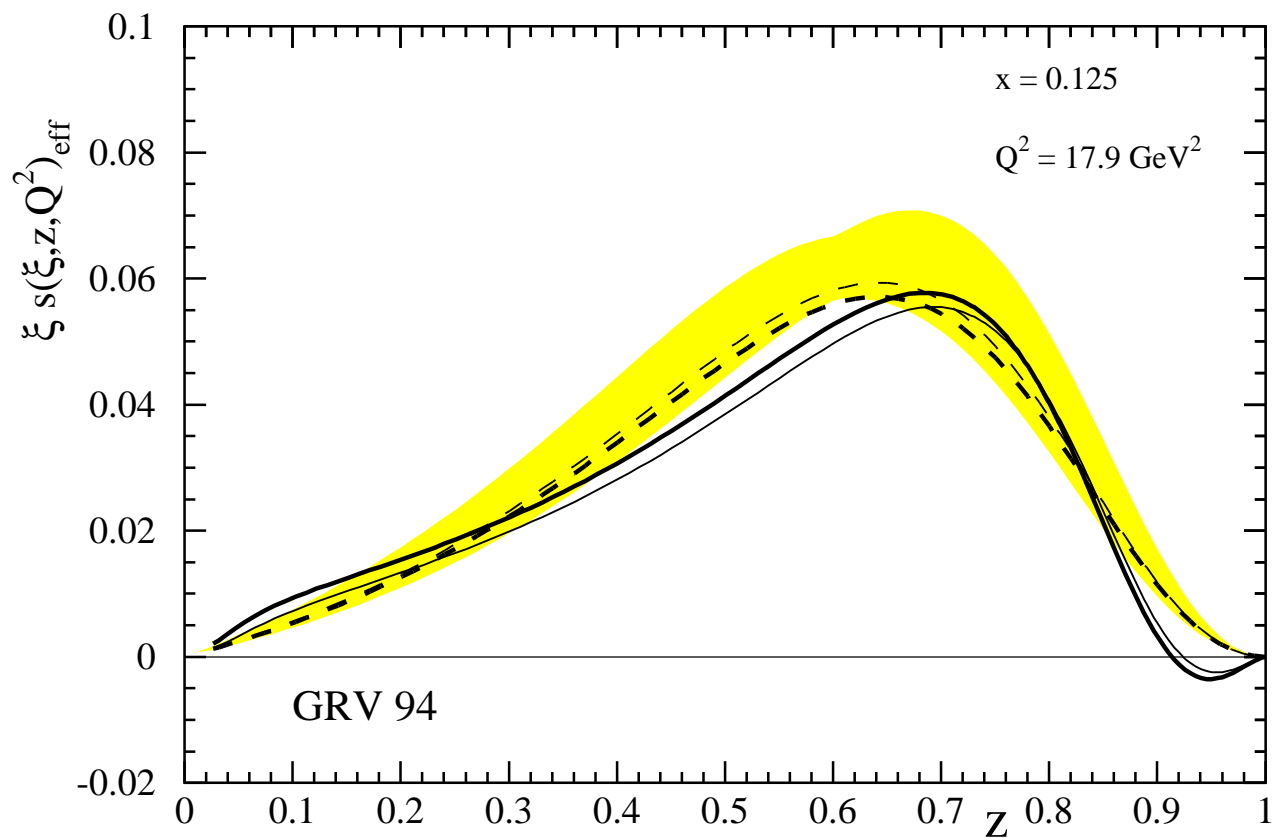
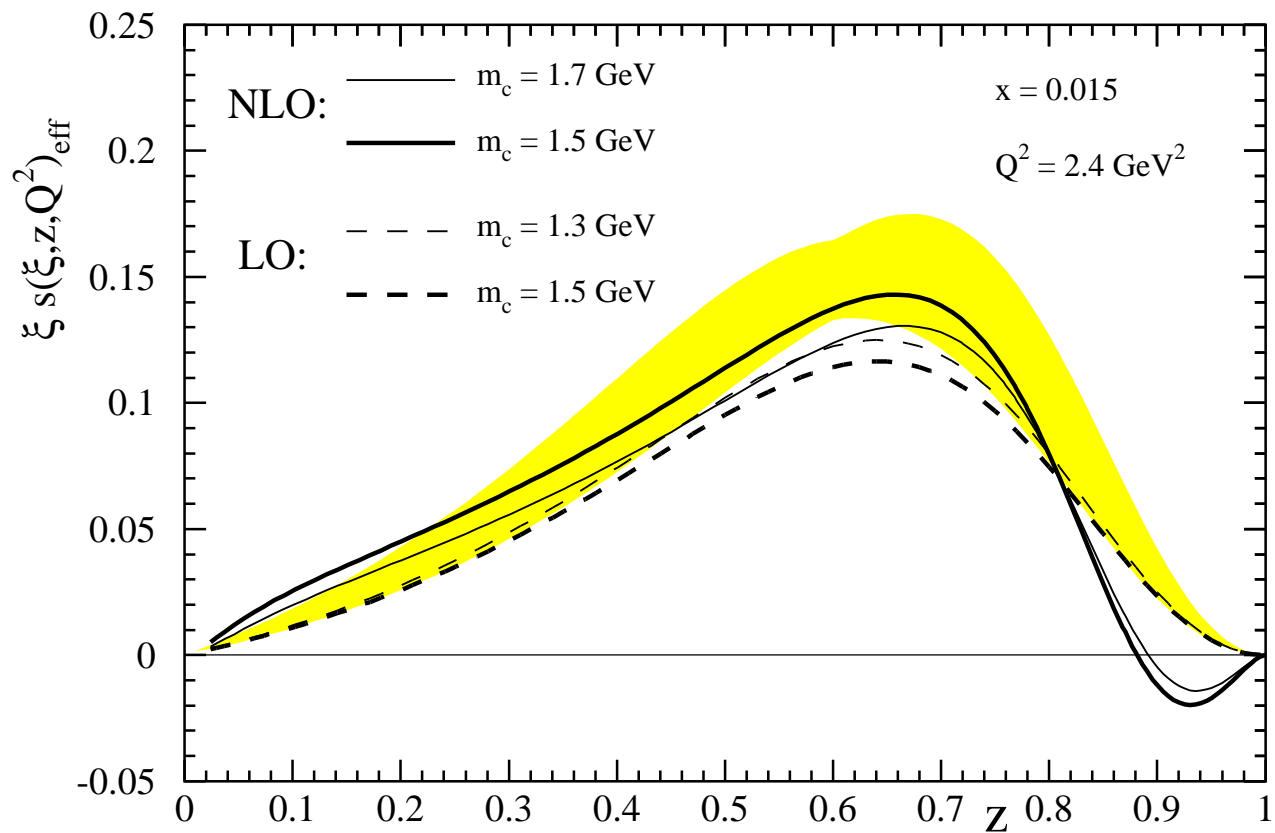


Fig. 3

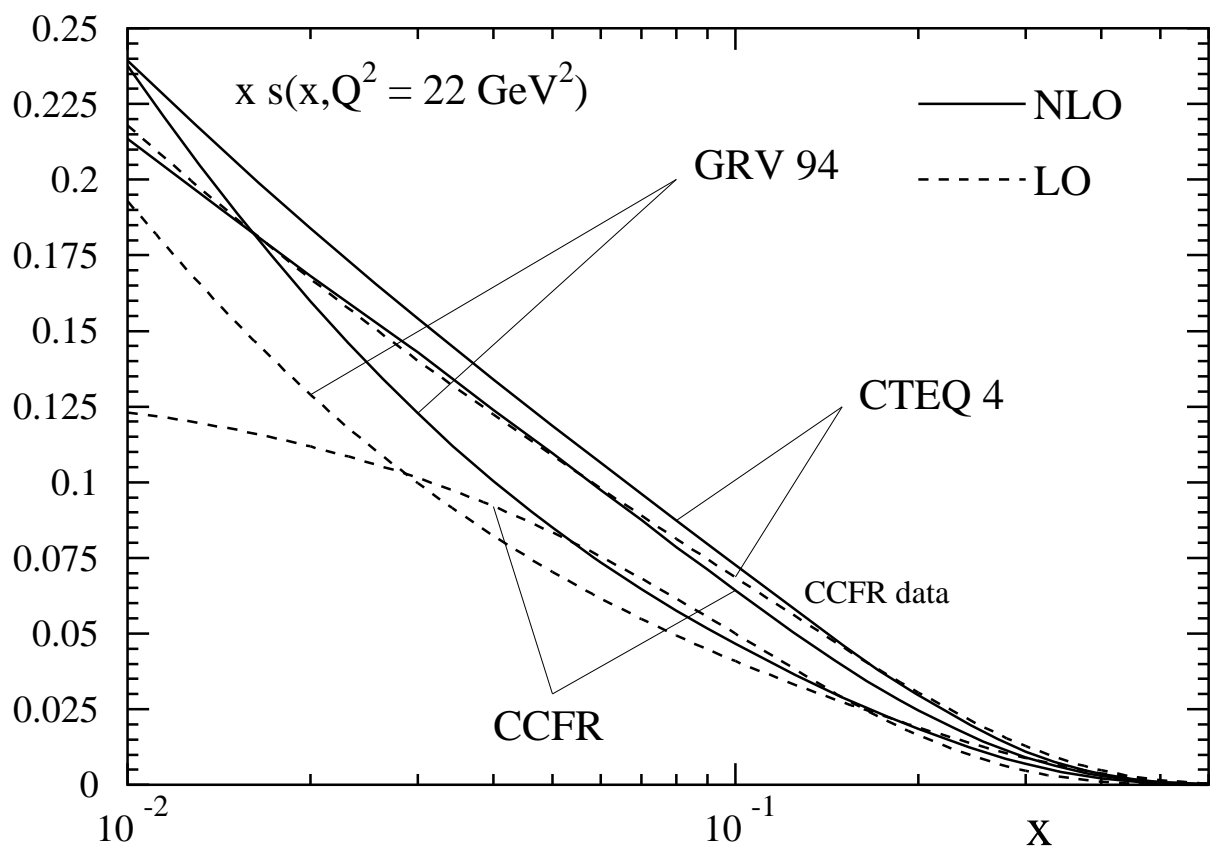
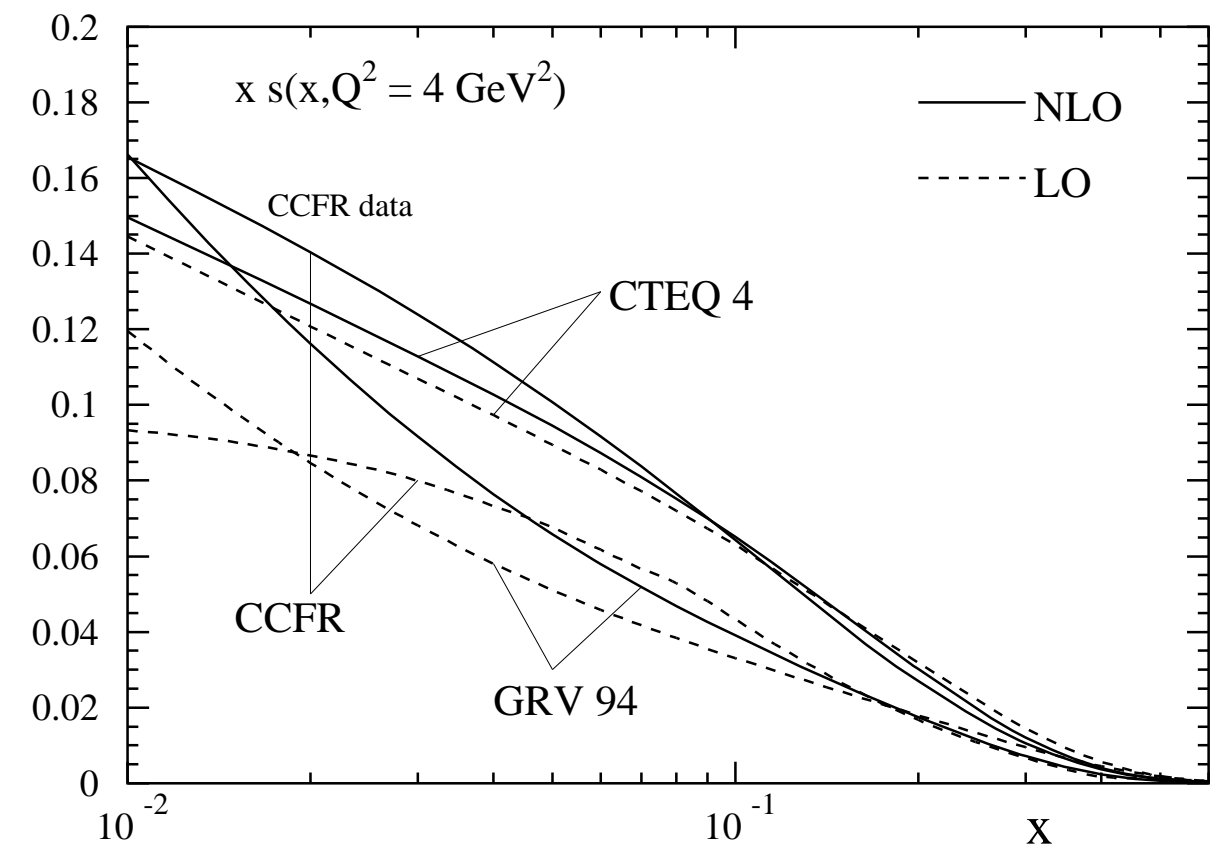


Fig. 4